Control Framework for Slung Load Transportation with Two Aerial Vehicles

Pedro O. Pereira and Dimos V. Dimarogonas

***Abstract*— We model a point mass load tethered to two aerial vehicles, and propose a control strategy that guarantees that the load tracks a desired position trajectory. Our framework consists in designing an input and a state transformation which converts the quadrotors-load system into three decoupled subsystems: one concerning the position of the load, with dynamics similar to those of an under-actuated aerial vehicle; one concerning the angle between the cables, with double integrator dynamics; and another concerning the yaw motion of the plane formed by the cables, also with double integrator dynamics. Once the decoupling is done, controllers from the literature can be leveraged, which we take advantage of when controlling the subsystem with dynamics similar to those of an under-actuated aerial vehicle. Simulations are presented which validate the proposed algorithm.**

I. Introduction

Execution of complex manipulation tasks with aerial vehicles is an active topic of research in robotics. Compared to ground robots, aerial robots allow for manipulation tasks to be executed in difficult to access spaces, paving the way to new applications, such as the inspection and maintenance of aging infrastructures [1].

Multi-rotor helicopters have been used to perform complex autonomous tasks [2], including manipulation tasks with grippers, robotic arms and cables [3]–[10]. Quadrotors, in particular, are preferred to others types of UAVs owing to their capability to hover, to take off and land vertically, to their high manoeuvrability, and to the availability of inexpensive components.

In this manuscript, we focus on the problem of transporting a load in a system composed of one load and two quadrotors, and where each quadrotor is connected to the load by a cable of fixed length. Grippers and robotic arms, when compared to cables, are expensive and mechanically complex, which motivates the study of tethered transportation. Moreover, transportation with multiple aerial vehicles adds robustness for when one or more team members suffers a failure, such as an actuator failure [3]. A model of this system, also referred to as slung load system, is found in [11], and controllers for position trajectory tracking of the load are found in the literature [8], [12]–[17]. Controllers for helicopters with experimental validation are found in [12], [13], where vision was used to estimate the state used in the feedback loop. For quadrotors, controllers are found in [8], [14]–[18], which explore differential flatness for planning trajectories mininizing sway; or which explore the dynamics to design controllers based on Lyapunov methods, such as backstepping. Adaptive strategies that compensate for the presence of unmodeled or unknown parameters, such as the load's mass or the cables lengths, are also found [19], [20].

The authors are with the School of Electrical Engineering, KTH Royal Institute of Technology, SE-100 44, Stockholm, Sweden. Email addresses: {ppereira, dimos}@kth.se. This work was supported by the EU H2020 Research and Innovation Programme under GA No.644128 (AEROWORKS), the Swedish Research Council (VR), the Swedish Foundation for Strategic Research (SSF) and the KAW Foundation.

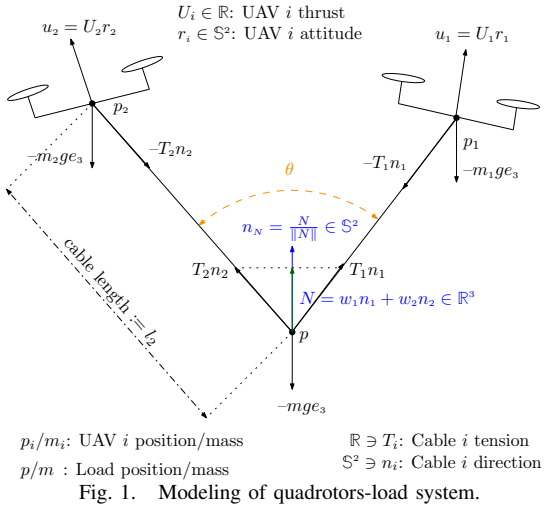

Fig. 1. Modeling of quadrotors-load system.

In this paper, we propose a control framework for trajectory tracking of the load. While in the literature specific control laws are found [3], [12], [17], we instead provide a general framework that transforms the quadrotors-load system into three decoupled subsystems, for which controllers are found in the literature. One of the subsystems, concerning the load's position, has the dynamics of an under-actuated aerial vehicle, which allows us to leverage hierarchical controllers for VTOL vehicles [21]. The other two subsystems, concerning the angle between the cables and the yaw position of the plane formed by the cables, have double integrator dynamics, for which controllers are also found in the literature. One of the control design challenges relates to the fact that a continuous controller defined over the whole state space cannot be found (for example, not defined when the cables overlap). One of the paper's contributions is to make explicit the domain where the control strategy is defined, and to provide specific control laws that guarantee that a solution never exits that domain.

II. Notation

The map $\mathcal{S} : \mathbb{R}^3 \ni x \mapsto \mathcal{S}(x) \in \mathbb{R}^{3\times 3}$ yields a skew-symmetric matrix and it satisfies $\mathcal{S}(a)\, b := a \times b$, for any $a, b \in \mathbb{R}^3$. $\mathbb{S}^2 := \{x \in \mathbb{R}^3 : x^T x = 1\}$ denotes the set of unit vectors in $\mathbb{R}^3$. The map $\Pi : \mathbb{S}^2 \ni x \mapsto \Pi(x) := I_3 - xx^T \in \mathbb{R}^{3\times 3}$ yields a matrix that represents the orthogonal projection onto the subspace perpendicular to $x \in \mathbb{S}^2$. We denote by $e_1, \cdots, e_n \in \mathbb{R}^n$ the canonical basis vectors in $\mathbb{R}^n$; when clear from the context, n is omitted. For some set A, id_A denotes the identity map on that set. Given some normed spaces A and B, and a function $f : A \ni a \mapsto f(a) \in B$, $Df : A \ni a \mapsto Df(a) \in \mathcal{L}(A, B)$ denotes the derivative

of f ($D_i f(a_1, \cdots, a_n)$ denotes the derivative w.r.t. the ith argument). Given a manifold A, $T_a A$ denotes the tangent set of A at some $a \in A$. In [22], the reader finds all the details and proofs, some of which we omit in this manuscript due to space constraints.

III. Modeling and Problem Statement

Consider two aerial vehicles, in particular quadrotor vehicles, and a point mass load attached to each quadrotor by a cable, as illustrated in Fig. 1. We denote by $p_1, p_2, p \in \mathbb{R}^3$ and by $v_1, v_2, v \in \mathbb{R}^3$ the quadrotors' and the load's center of mass positions and velocities, respectively; by $m_1, m_2, m > 0$ the quadrotor's and load's masses, respectively; and by $l_1, l_2 > 0$ the cables' lengths. Finally, we denote by $u_1, u_2 \in \mathbb{R}^3$ the quadrotors' input forces, which we assume are inputs to the quadrotors-load system. In [22], we let the quadrotors' attitude (i.e., $r_1, r_2 \in \mathbb{S}^2$) be part of the state, and we assume we have control over the quadrotors thrusts and angular velocities (i.e., $U_1, U_2 \in \mathbb{R}$ and $\omega_{r_1}, \omega_{r_2} \in \mathbb{R}^3$). Consider then the state space $\mathbb{Z}$ in (1); hereafter we always decompose a $z \in \mathbb{Z}$ and a $u \in \mathbb{R}^6$ in the same way, namely, $u \in \mathbb{R}^6 :\Leftrightarrow (u_1, u_2) \in (\mathbb{R}^3)^2$ and

$$z \in \mathbb{Z} :\Leftrightarrow (z_k, z_d) \in \mathbb{Z} :\Leftrightarrow (p, v, p_1, v_1, p_2, v_2) \in \mathbb{Z}, \quad (3)$$

with $z_k \in \mathbb{Z}_k$. We use a z as in (3) to represent the state of the system, where z_k collects all the kinematic (position) variables of the quadrotors-load system, while z_d collects all the dynamic (velocity) variables. The state space definition in (1) allows for the definition of the cables' unit vectors, namely, for $i \in \{1, 2\}$, we define

$$\mathbb{Z}_k \ni z_k \mapsto n_i(z_k) := \frac{p_i - p}{\|p_i - p\|} \overset{(1)}{=} \frac{p_i - p}{l_i} \in \mathbb{S}^2, \quad (4)$$

where (4) can be visualized in see Fig. 1.

Given an appropriate $u : \mathbb{R}_{\geq 0} \mapsto \mathbb{R}^6$, a system's trajectory $z : \mathbb{R}_{\geq 0} \ni t \mapsto z(t) \in \mathbb{Z}$ evolves according to

$$\dot{z}(t) = Z(z(t), u(t)), z(0) \in \mathbb{Z}, \quad (5)$$

where $Z : \mathbb{Z} \times \mathbb{R}^6 \ni (z, u) \mapsto Z(z, u) \in \mathbb{R}^{18}$ is given by

$$Z(z,u) := \begin{bmatrix} Z_k(z_d) \\ Z_d(z,u) \end{bmatrix} \left(= \begin{bmatrix} \dot{z}_k \\ \dot{z}_d \end{bmatrix} \right), \quad (6)$$

$$Z_k(z_d) := z_d = \begin{bmatrix} v \\ v_1 \\ v_2 \end{bmatrix} \left(= \begin{bmatrix} \dot{p} \\ \dot{p}_1 \\ \dot{p}_2 \end{bmatrix} \right),$$

$$Z_d(z,u) := \begin{bmatrix} \sum_{i\in\{1,2\}} \frac{T_i(z,u)}{m} n_i(z) - g e_3 \\ \frac{u_1}{m_1} - \frac{T_1(z,u)}{m_1} n_1(z) - g e_3 \\ \frac{u_2}{m_2} - \frac{T_2(z,u)}{m_2} n_2(z) - g e_3 \end{bmatrix} \left(= \begin{bmatrix} \dot{v} \\ \dot{v}_1 \\ \dot{v}_2 \end{bmatrix} \right), \quad (7)$$

where g stands for the acceleration due to gravity, and T_1 and T_2 stand for the tensions in the cables (which are functions of the state and the input). The accelerations in (7) are written based the Newton's equations of motion, considering the net force on each point mass, as illustrated in Fig. 1. However, the latter equations do not provide any insight about the tensions T_1 and T_2, since they are internal forces. The constraint that any trajectory of (5) must be contained in $\mathbb{Z}$, enforces the vector field (6) to be in the tangent set of $\mathbb{Z}$, i.e., in $T_{z\in\mathbb{Z}}\mathbb{Z}$ (this set is found in [22], and is here omitted for brevity). This constraint uniquely defines the tensions, i.e., for any $(z, u) \in \mathbb{Z} \times \mathbb{R}^6$, (2) follows. The vector field (6) may also be derived by means of the Euler-Lagrange formalism [15]. Notice that the quadrotors-load system has a 7th dimensional generalized coordinate (three coordinates for the load's position, and two coordinates for each cable unit vector), while the input to the system is only 6th dimensional. That means that the quadrotors-load system is under-actuated. Let us now state the problem to be solved in this paper.

Problem 1: Given a desired smooth position trajectory $p^\star \in \mathbb{R}_{\geq 0} \mapsto \mathbb{R}^3$, design $u = (u_1, u_2) : \mathbb{R}_{\geq 0} \mapsto \mathbb{R}^6$ such that $\lim_{t\to\infty}(p(t) - p^\star(t)) = 0$ along trajectories of (5).

We emphasize that the vector field (6) is input affine, i.e., that $Z(z, u) = A(z) + \begin{bmatrix} 0^T_{9\times 6} & B(z_k)^T \end{bmatrix}^T u$ for some $A(z) \in \mathbb{R}^{18}$ and $B(z_k) \in \mathbb{R}^{9\times 6}$ (found in [22] – we emphasize that the B matrix depends only on the kinematic variables).

IV. Control Law Design

A. Control Strategy

Let us explain the pursued control strategy, which is illustrated in Fig. 2. As a first step, we introduce an input transformation from $\nu := (\nu_1, \nu_2, \nu_3) \in \mathbb{R}^{4+1+1}$ to $u \in \mathbb{R}^6$. Intuitively, $\nu_1 \equiv (T, \tau) \in \mathbb{R}^{1+3}$ where T will stand for the force along the direction of N in Fig. 1, while τ will stand for the angular acceleration of the unit vector associated to N; and we design ν_1 to control the position of the load. On the the other hand, $\nu_2 \equiv \tau_\theta \in \mathbb{R}$ will stand for the acceleration of the angle between the cables (θ in Fig. 1), and we will design ν_2 to control that angle. And, finally, $\nu_3 \equiv \tau_\psi \in \mathbb{R}$ will stand for the acceleration of the yaw position associated to the plane formed by the two cables, and we will design ν_3 to control that yaw position. The idea is that $\nu := (\nu_1, \nu_2, \nu_3)$ provides a more meaningful input to design, and once it is designed, one can map ν to u (the actual input) by means of the function $\bar{u}$ (see Fig. 2). This is done in Section IV-C.

In the second step, done in Section IV-D, we provide a coordinate transformation g that maps a $z \in \tilde{\mathbb{Z}} \subset \mathbb{Z}$ into an $x \in \tilde{\mathbb{X}}$ (g, $\tilde{\mathbb{Z}}$ and $\tilde{\mathbb{X}}$ are defined later), and with this coordinate transformation, we obtain a new vector field, which comes from the composition of the state transformation with the vector field Z in (6) and the input transformation. In fact, this new vector field is composed of three decouple vector fields, namely X_1, X_2 and X_3, where each vector field has as an input ν_1, ν_2 and ν_3, respectively (see Fig. 2). The

$$\mathbb{Z} = \left\{(p, p_1, p_2, v, v_1, v_2) \in (\mathbb{R}^3)^6 : (p, p_1, p_2) \in \mathbb{Z}_k, i \in \{1, 2\}, (v_i - v)^T (p_i - p) = 0\right\}, \quad (1)$$
$$\mathbb{Z}_k = \left\{(p, p_1, p_2) \in (\mathbb{R}^3)^3 : i \in \{1, 2\}, (p_i - p)^T (p_i - p) = l_i^2\right\},$$

$$Z(z,u) \in T_z\mathbb{Z} \Rightarrow \begin{bmatrix} T_1(z,u) \\ T_2(z,u) \end{bmatrix} = \underbrace{\begin{bmatrix} \frac{m}{m_1} + 1 & c \\ c & \frac{m}{m_2} + 1 \end{bmatrix}^{-1} \left(\begin{bmatrix} \frac{m}{m_1} n_1(z_k)^T & 0_{1\times 3} \\ 0_{1\times 3} & \frac{m}{m_2} n_2(z_k)^T \end{bmatrix} \begin{bmatrix} u_1 \\ u_2 \end{bmatrix} + m \begin{bmatrix} \frac{\|v_1 - v\|^2}{l_1} \\ \frac{\|v_2 - v\|^2}{l_2} \end{bmatrix} \right)}_{=:M_T(z_k)\in\mathbb{R}^{2\times 6}} \Big|_{c = n_1(z_k)^T n_2(z_k)}. \quad (2)$$

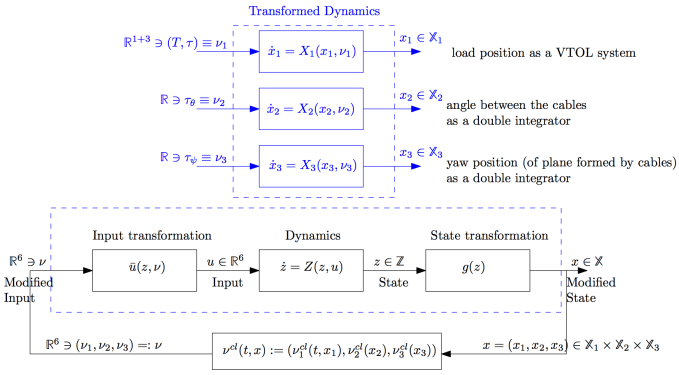

Fig. 2. Control strategy: the vector field (6) is decomposed into three decoupled vector fields, by means of an input and state transformation.

benefit of this coordinate transformation is that it highlights the decoupled structure of the problem, and thus it allows us to design control laws for ν_1, ν_2 and ν_3 separately. One of our main contributions is to show that the vector field X_1 is one for which controllers already exist in the literature.

In the final step, done in Section V, we present control laws $\mathbb{R}_{\geq 0} \times \tilde{\mathbb{X}}_1 \ni (t, x_1) \mapsto \nu_1^{cl}(t, x_1) \in \mathbb{R}^4$, $\tilde{\mathbb{X}}_2 \ni x_2 \mapsto \nu_2^{cl}(x_2) \in \mathbb{R}$ and $\tilde{\mathbb{X}}_3 \ni x_3 \mapsto \nu_3^{cl}(x_3) \in \mathbb{R}$ and combine them to define $\tilde{\mathbb{X}} := \tilde{\mathbb{X}}_1 \times \tilde{\mathbb{X}}_2 \times \tilde{\mathbb{X}}_3$ and $\mathbb{R}_{\geq 0} \times \tilde{\mathbb{X}} \ni (t, x) \mapsto \nu^{cl}(t, x) \in \mathbb{R}^6$ as

$$\nu^{cl}(t, x) := (\nu_1^{cl}(t, x_1), \nu_2^{cl}(x_2), \nu_3^{cl}(x_3)), \tag{8}$$

which guarantees that Problem 1 is accomplished and that $\tilde{\mathbb{X}}$ is positively invariant. Finally, using the mapping $\bar{u}$, one constructs the control law for the original system, i.e., $\mathbb{R}_{\geq 0} \times \tilde{\mathbb{Z}} \ni (t, z) \mapsto u^{cl}(t, z) \in \mathbb{R}^6$ defined as

$$u^{cl}(t, z) := \bar{u}(z, \nu^{cl}(t, x))|_{x=g(z)}, \tag{9}$$

which yields the closed loop vector field

$$\mathbb{R}_{\geq 0} \times \tilde{\mathbb{Z}} \ni (t, z) \mapsto Z^{cl}(t, z) := Z(z, u^{cl}(t, z)) \in \mathbb{R}^{18}. \tag{10}$$

One of the challenges in the control design is to guarantee that a solution $t \mapsto z(t)$ of $\dot{z}(t) = Z^{cl}(t, z(t))$ remains in $\{z \in \tilde{\mathbb{Z}} : g(z) \in \tilde{\mathbb{X}}\} \subset \mathbb{Z}$ which is the set where the control law (9) is well defined.

B. Preliminary Definitions

We are interested in controlling the position of the load, the angle between the cables and the yaw position of the plane defined by the cables, where we emphasize that these quantities depend exclusively on the kinematic variables ($z_k := (p, p_1, p_2) \in \mathbb{Z}_k$). With that in mind, and in order to construct the input and coordinate transformation illustrated in Fig 2, we must define the first and second derivatives of smooth functions in $\mathbb{Z}_k$, or, more generally, in a subset of $\mathbb{Z}_k$ which we denote here by $\tilde{\mathbb{Z}}_k$ (denote also $\tilde{\mathbb{Z}} := \{(z_k, z_d) \in \mathbb{Z} : z_k \in \tilde{\mathbb{Z}}_k\} \subset \mathbb{Z}$). Consider then a smooth function $f : \tilde{\mathbb{Z}}_k \ni z_k \mapsto f(z_k) \in \mathbb{R}^n$ for some $n \in \mathbb{N}$. We denote

$$f^{(1)} : \tilde{\mathbb{Z}} \ni (z_k, z_d) \mapsto f^{(1)}(z_k, z_d) (= \dot{f}(z_k)) \in \mathbb{R}^n,$$
$$f^{(2)} : \tilde{\mathbb{Z}} \times \mathbb{R}^6 \ni (z, u) \mapsto f^{(2)}(z, u) (= \ddot{f}(z_k)) \in \mathbb{R}^n,$$

as the first and second derivatives of f along the vector field (6) (their explicit expression is found in [22]). We only note here that, because the vector field is input affine, then $f^{(2)}$ can be expressed as

$$f^{(2)}(z, u) := A_f(z) + B_f(z_k)u. \tag{11}$$

for some $A_f(z) \in \mathbb{R}^n$ and $B_f(z_k) \in \mathbb{R}^{n \times 6}$ found in [22]. Suppose now that $f : \tilde{\mathbb{Z}}_k \in z_k \mapsto f(z_k) \in \mathbb{R}^3 \backslash \{0_3\}$ We can then define

$$n_f : \tilde{\mathbb{Z}}_k \ni z_k \mapsto n_f(z_k) := \frac{f(z_k)}{\|f(z_k)\|} \in \mathbb{S}^2, \tag{12}$$
$$\omega_f : \tilde{\mathbb{Z}} \ni (z_k, z_d) \mapsto \omega_f(z_k, z_d) (= \mathcal{S}(n(z_k))\, \dot{n}(z_k)) \in \mathbb{R}^3,$$
$$\tau_f : \tilde{\mathbb{Z}} \times \mathbb{R}^6 \ni (z, u) \mapsto \tau_f(z, u) (= \dot{\omega}(z_k, z_d)) \in \mathbb{R}^3, \tag{13}$$

where n_f is the unit vector associated to the function f, ω_f is the angular velocity of n_f, and finally τ_f is the angular acceleration of n_f. Once again, because the vector field is input affine, then τ_f can be expressed as

$$\tau_f(z, u) = A_{n_f}(z) + B_{n_f}(z_z)u, \tag{14}$$

for some $A_{n_f}(z) \in \mathbb{R}^3$ and $B_{n_f}(z_z) \in \mathbb{R}^{3 \times 6}$ (found in [22]).

C. Input Transformation

Let us now provide the input transformation $\bar{u}$ illustrated in Fig. 2. For that purpose we introduce a function

$$R : \tilde{\mathbb{Z}} \times \mathbb{R}^6 \ni (z, u) \mapsto R(z, u) \in \mathbb{R}^m \tag{15}$$

of $m \in \mathbb{N}$ *physical quantities* we wish to regulate/control, where $\tilde{\mathbb{Z}}$ is a subset of $\mathbb{Z}$ (where the controller is defined). In particular, we wish to control 6 quantities: the force (or linear acceleration) along the direction of N represented in Fig. 1 (2 quantities [22]); the angular acceleration of the unit vector associated to N (2 quantities: the angular acceleration is three dimensional, but orthogonal to N); the angular acceleration of the angle between the cables (1 quantity, which we will name $\tau_\theta \in \mathbb{R}$); and finally the angular acceleration on the yaw position (1 quantity, which we will name $\tau_\psi \in \mathbb{R}$). With the above in mind, let us define

$$\mathbb{Z}_{k,N} := \{z_k \in \mathbb{Z}_k : n_1(z_k)^T n_2(z_k) \neq -1\}, \tag{16}$$
$$N : \mathbb{Z}_{k,N} \ni z_k \mapsto N(z_k) := w_1 n_1(z_k) + w_2 n_2(z_k) \in \mathbb{R}^3 \backslash \{0_3\},$$

as the vector N represented in Fig 1, for some positive convex weights w_1 and w_2 ($w_1 + w_2 = 1$; see Remark 1). We introduced in Section IV-B, how to compute the unit vector associated to N and its angular velocity and acceleration, namely n_N, ω_N and τ_N (see (12)–(13) and (14)). Define also

$$\mathbb{Z}_{k,\theta} := \{z_k \in \mathbb{Z}_k : n_1(z_k)^T n_2(z_k) \neq \pm 1\}, \tag{17}$$
$$\theta : \mathbb{Z}_{k,\theta} \ni z_k \mapsto \theta(z_k) := \arccos(n_1(z_k)^T n_2(z_k)) \in (0, \pi), \tag{18}$$

as the angle between the cables, represented in Fig 1. We introduced in Section IV-B how to compute the velocity and acceleration of θ, namely $\theta^{(1)}$ and $\theta^{(2)}$. Finally define (below, denote $\delta(z_k) \equiv \Pi(e_3)(n_1(z_k) - n_2(z_k))$, $c \equiv \frac{e_1^T \delta(z_k)}{\|\delta(z_k)\|}$ and $s \equiv \frac{e_2^T \delta(z_k)}{\|\delta(z_k)\|}$)

$$\mathbb{Z}_{k,\psi} := \{z_k \in \mathbb{Z}_k : \|\delta(z_k)\| > 0\},$$
$$\psi : \mathbb{Z}_{k,\psi} \ni z_k \mapsto \psi(z_k) := \tfrac{1}{2} \arctan(c^2 - s^2, 2cs) \in \left[-\tfrac{\pi}{2}, \tfrac{\pi}{2}\right], \tag{19}$$

as the yaw position of the plane formed by the cables. We introduced in Section IV-B how to compute the velocity and

acceleration of ψ, namely $\psi^{(1)}$ and $\psi^{(2)}$ (details on the co-domain of ψ in (19) are found in [22]). For convenience, define (which will become clear next),

$$\mathbb{Z}_{k,\text{inv}} := \{z_k \in \mathbb{Z}_k : e_3^T n_{i\in\{1,2\}}(z_k) > 0, n_1(z_k)^T n_2(z_k) > 0\}, \quad (20)$$

With the above in mind, define the function R in (15), with

$$\tilde{\mathbb{Z}}_k := \mathbb{Z}_{k,N} \cap \mathbb{Z}_{k,\theta} \cap \mathbb{Z}_{k,\psi} \cap \mathbb{Z}_{k,\text{inv}}, \quad (21)$$

$$\tilde{\mathbb{Z}} := \{z := (z_k, z_d) \in \mathbb{Z} : z_k \in \tilde{\mathbb{Z}}_k\}, \quad (22)$$

and as (below $\sum \equiv \sum_{i\in\{1,2\}}$)

$$R(z,u) := \begin{bmatrix} \frac{1}{m}\sum T_i(z,u) n_i(z_k) \\ \tau_N(z,u) \\ \theta^{(2)}(z,u) \\ \psi^{(2)}(z,u) \end{bmatrix} \overset{\substack{(2)\\(14)\\(11)}}{=} \underbrace{\begin{bmatrix} \frac{1}{m}\sum T_i(z,0_6) \\ A_{n_N}(z) \\ A_\theta(z) \\ A_\psi(z) \end{bmatrix}}_{=:A_R(z)\in\mathbb{R}^6} + \underbrace{\begin{bmatrix} \frac{1}{m}\sum n_i(z_k) e_1^T M_T(z_k) \\ B_{n_N}(z_k) \\ B_\theta(z_k) \\ B_\psi(z_k) \end{bmatrix}}_{=:B_R(z_k)\in\mathbb{R}^{6\times 6}} \begin{bmatrix} u_1 \\ u_2 \end{bmatrix}.$$

Denote $\nu = (T, \tau_N, \tau_\theta, \tau_\psi) \in \mathbb{R}^{1+3+1+1}$, and given any $z \in \tilde{\mathbb{Z}}$ define $\bar{\nu}(z,\nu) := (T n_N(z_k), \Pi\left(n_N(z_k)\right)\tau_N, \tau_\theta, \tau_\psi)$. We note that there exists a unique $\bar{u} : \tilde{\mathbb{Z}} \times \mathbb{R}^6 \ni (z,\nu) \mapsto \bar{u}(z,\nu) \in \mathbb{R}^6$ such that $\bar{\nu}(z,\nu) = R(z, \bar{u}(z,\bar{\nu}(z,\nu)))$ and it is given by

$$\bar{u}(z,\nu) := (B_R(z_k)^T B_R(z_k))^{-1} B_R(z_k)^T (\bar{\nu}(z,\nu) - A_R(z)), \quad (23)$$

Notice that there exists an inverse on (23), which depends exclusively on the kinematic configuration, and it can be shown that (23) is well defined for any $z_k \in \tilde{\mathbb{Z}}_k$ with $\tilde{\mathbb{Z}}_k$ as in (22): $\mathbb{Z}_{k,N} \cap \mathbb{Z}_{k,\theta} \cap \mathbb{Z}_{k,\psi}$ is necessary as the domain where N, θ and ψ are defined, while $\mathbb{Z}_{k,\text{inv}}$ is necessary for invertibility [22].

Remark 1: Suppose we wish the load to be at a constant position. One can compute the equilibria state and input, i.e., $\bar{z} \in \mathbb{Z}$ and $\bar{u} \in \mathbb{R}^6$ for which $Z(\bar{z},\bar{u}) = 0_{18}$, and it holds that $\frac{T_1(\bar{z},\bar{u})}{T_2(\bar{z},\bar{u})} = \frac{w_1}{w_2}$. Thus, the ratio $\frac{w_1}{w_2}$ determines the weight distribution of the load onto each UAV.

D. State Transformation

Let us now provide the coordinate transformation illustrated in Fig. 2, which will expose the three decoupled problems illustrated in that figure. Define then the state sets

$$\mathbb{X}_1 := \{x_1 := (p, v, n, \omega) \in (\mathbb{R}^3)^4 : n \in \mathbb{S}^2, \omega^T n = 0\}, \quad (24a)$$

$$\mathbb{X}_2 := \{x_2 := (\theta, \omega_\theta) \in \mathbb{R}^2 : \theta \in (0, \pi)\},$$

$$\mathbb{X}_3 := \{x_3 := (\psi, \omega_\psi) \in \mathbb{R}^2\}. \quad (24b)$$

We always decompose an $x_1 \in \mathbb{X}_1$, an $x_2 \in \mathbb{X}_2$ and an $x_3 \in \mathbb{X}_3$ as decomposed in (24a)–(24b). Consider then the mapping $\mathbb{Z} \ni z \mapsto g(z) \in \mathbb{X}_1 \times \mathbb{X}_2 \times \mathbb{X}_3$ defined as

$$g(z) := (g_1(z), g_2(z), g_3(z)) \quad (25a)$$

$$g_1(z) := (p, v, n_N(z_k), \omega_N(z_k, z_d)) \in \mathbb{X}_1, \quad (25b)$$

$$g_2(z) := (\theta(z_k), \theta^{(1)}(z_k, z_d)) \in \mathbb{X}_2, \quad (25c)$$

$$g_3(z) := (\psi(z_k), \psi^{(1)}(z_k, z_d)) \in \mathbb{X}_3, \quad (25d)$$

where g_1 in (25b) isolates the position, the velocity, the unit vector given by N (see Fig. 1) and its angular velocity; g_2 in (25c) isolates the angle between the cables, and its angular velocity; and g_3 in (25d) isolates the yaw position and its angular velocity (all the functions in (25b)–(25d) are those introduced in Sections IV-C and IV-B). The mapping g in (25a) is invertible (in a subset $\tilde{\mathbb{X}}_3$ we introduce later), but we can proceed without having to compute its inverse.

It follows after simple calculations that (denote $\nu_1 := (T, \tau) \in \mathbb{R}^{1+3}$)

$$Dg_1(z)Z(z,\bar{u}(z,\nu)) = \begin{bmatrix} v \\ T n_N(z_k) - g e_3 \\ \mathcal{S}\left(\omega_N(z_k,z_d)\right) n_N(z_k) \\ \Pi\left(n_N(z_k)\right)\tau \end{bmatrix} \left(= \begin{bmatrix} \dot{p} \\ \dot{v} \\ \dot{n}_N \\ \dot{\omega}_N \end{bmatrix}\right) \quad (26a)$$

$$Dg_2(z)Z(z,\bar{u}(z,\nu)) = \begin{bmatrix} \theta^{(1)}(z_k, z_d) \\ \tau_\theta \end{bmatrix} \left(= \begin{bmatrix} \dot{\theta} \\ \dot{\omega}_\theta \end{bmatrix}\right), \quad (26b)$$

$$Dg_3(z)Z(z,\bar{u}(z,\nu)) = \begin{bmatrix} \psi^{(1)}(z_k, z_d) \\ \tau_\psi \end{bmatrix} \left(= \begin{bmatrix} \dot{\psi} \\ \dot{\omega}_\psi \end{bmatrix}\right). \quad (26c)$$

The choice of the control input (23) and the mappings (25b)–(25d) is now clear: it induces three decoupled vector fields, namely those in (26a), (26b) and (26c). The vector fields (26b) and (26c) are those of double integrators, while the vector field in (26a) is that of a thrust propelled system. Since these vector fields are decoupled, we can design control laws for $\nu_1 \equiv (T, \tau)$, $\nu_2 \equiv \tau_\theta$ and $\nu_2 \equiv \tau_\psi$ separately.

V. Separate Control Laws

We must now develop three control laws for the three decoupled systems, as illustrated in Fig. 2. Recall however that the mapping $\bar{u}$ in (23) – illustrated in Fig. 2 and which allows for the decoupling – is only well defined for a subset of the kinematic space. Indeed, it is well defined for all $z \in \tilde{\mathbb{Z}} \Leftrightarrow z_k \in \tilde{\mathbb{Z}}_k$ (see (21) and (22)). As such, the control design idea that we follow next is to assume that $z_k(0) \in \tilde{\mathbb{Z}}_k$, and to develop controllers which guarantee that $z_k(t) \in \tilde{\mathbb{Z}}_k$ for all $t \geq 0$, thus guaranteeing well-posedness of the control law.

A. Control of angle between the cables

We start with the control design for the angle between the cables, which we want to converge to some $\theta^\star \in (0, \frac{\pi}{4})$. Recall then the vector field (26b), which can be written as $\mathbb{X}_2 \ni x_2 \mapsto X_2(x_2, \tau_\theta) = (\omega_\theta, \tau_\theta) \in \mathbb{R}^2$, and that our goal is to guarantee that z_k remains in $\tilde{\mathbb{Z}}_k$ in (21). The set $\mathbb{Z}_{k,\theta}$ in (17) motivates the definition of

$$\tilde{\mathbb{X}}_2 := \left\{(\theta, \omega_\theta) \in \mathbb{X}_2 : \theta \in \left(0, \frac{\pi}{4}\right)\right\}. \quad (27)$$

The lower bound 0 in (27) is needed because the mapping $\bar{u}$ is not well defined when the cables overlap; the upper bound $\frac{\pi}{4}$ can only be understood in Section V-B, and it guarantees that the first two conditions in (20) are satisfied. Consider the following control law $\tilde{\mathbb{X}}_2 \ni x_2 \mapsto \tau_\theta^{cl}(x_2) \in \mathbb{R}$ defined as

$$\nu_2^{cl}(x_2) \equiv \tau_\theta^{cl}(x_2) := -k_\theta \frac{\theta - \theta^\star}{\theta\left(\theta - \frac{\pi}{4}\right)} - k_{\omega_\theta}\omega_\theta, \quad (28)$$

which induces the closed loop vector field $\tilde{\mathbb{X}}_2 \ni x_2 \mapsto X_2^{cl}(x_2) := X_2(x_2, \tau_\theta^{cl}(x_2))$. We emphasize that $\tau_\theta^{cl}((\theta^\star, 0)) = 0$, that $\lim_{\theta\to 0} \tau_\theta^{cl}((\theta,\cdot)) = \infty$ and that $\lim_{\theta\to\pi/4} \tau_\theta^{cl}((\theta,\cdot)) = -\infty$. Moreover, it follows that for the

(Lyapunov) function $\tilde{\mathbb{X}}_2 \ni x_2 \mapsto V_2(x_2) \geq 0$ defined as $V_2(x_2) := k_\theta \int_{s=\theta^\star}^{s=\theta} \frac{s-\theta^\star}{s\left(s-\frac{\pi}{4}\right)} ds + \frac{1}{2}\omega_\theta^2$ it holds that $\tilde{\mathbb{X}}_2 \ni x_2 \mapsto W_2(x_2) := DV_2(x_2)X_2^{cl}(x_2)$ yields $W_2(x_2) := -k_{\omega_\theta}\omega_\theta^2 \leq 0$. It follows from V_2 and W_2 that a solution $t \mapsto x_2(t)$ of $\dot{x}_2(t) = X_2^{cl}(x_2(t))$ with $x_2(0) \in \tilde{\mathbb{X}}_2$ never gets arbitrarily close to the boundaries of $\tilde{\mathbb{X}}_2$ (i.e., θ never gets arbitrarily close to 0 or $\frac{\pi}{4}$); and that $\lim_{t\to\infty} x_2(t) = (\theta^\star, 0)$. For the quadrotors-load system this is equivalent to saying that the angle between the cables converges to a desired angle $\theta^\star \in (0, \frac{\pi}{4})$; and that it never gets arbitrarily close to 0 (and thus that the UAVs do not collide) or arbitrarily close to $\frac{\pi}{4}$, and thus that $0 < \theta(z_k) := \arccos(n_1(z_k)^T n_2(z_k)) < \frac{\pi}{4}$ which implies that (this implication can be easily understood from Fig. 1)

$$0 < \arccos(n_i(z_k)^T n_N(z_k)) < \pi/4, \tag{29}$$

which means that z_k remains in the sets $\mathbb{Z}_{k,N}$ and $\mathbb{Z}_{k,\theta}$ in (16) and (17).

B. Control of the thrust propelled system

Recall then the vector field (26a). Our goal is to guarantee that z_k remains in $\tilde{\mathbb{Z}}_k$ in (21), which motivates the definition

$$\tilde{\mathbb{X}}_1 := \left\{(p, v, n, \omega) \in \mathbb{X}_1 : n^T e_3 > \frac{\pi}{4}\right\}. \tag{30}$$

The vector field in (26a) is that of a thrust propelled vector field, for which controllers

$$\mathbb{R}_{\geq 0} \times \mathbb{X}_1 \ni (t, x_1) \mapsto \nu_1^{cl}(t, x_1) \equiv (T^{cl}(t, x_1), \tau^{cl}(t, x_1)) \in \mathbb{R}^4 \tag{31}$$

are found in the literature, which guarantee that $\lim_{t\to\infty} p(t) - p^\star(t) = 0_3$ (with $p^\star$ coming from Problem 1). Suppose moreover that the controller in (31) guarantees that the set $\tilde{\mathbb{X}}_1$ is positively invariant (this is possible with the controller found in [23]). Then, it follows from the triangular inequality that

$$\begin{aligned} n_i(z_k)^T e_3 &\geq \cos\left(\arccos(n_i(z_k)^T n(z_k)) + \arccos(n(z_k)^T e_3)\right) \\ &\overset{(30)}{\geq} \cos\left(\arccos(n_i(z_k)^T n(z_k)) + \tfrac{\pi}{4}\right) \overset{(29)}{\geq} \cos\left(\tfrac{\pi}{4} + \tfrac{\pi}{4}\right) > 0, \end{aligned}$$

which means that z_k satisfies the first two conditions in $\mathbb{Z}_{k,\text{inv}}$ in (20).

C. Control of yaw position

Consider now the vector field (26c), which can be written as $\mathbb{X}_3 \ni x_3 \mapsto X_3(x_3, \tau_\psi) := (\omega_\psi, \tau_\psi) \in \mathbb{R}^2$, and recall that our goal is to guarantee that z_k remains in $\tilde{\mathbb{Z}}_k$ in (21). Recall also (19), which motivates the definition

$$\psi_1 \sim \psi_2 :\Leftrightarrow \psi_1 - \psi_2 = k\pi, k \in \{\cdots, -1, 0, 1, \cdots\}, \tag{32}$$

where $\sim$ is an equivalence relation, namely (i.e., two angles are equivalent if they differ by a multiple of half of a full rotation). Denote $\tilde{\mathbb{X}}_3 := \mathbb{X}_3$, and consider then the control law $\tilde{\mathbb{X}}_3 \ni x_3 \mapsto \tau_\psi^{cl}(x_3) \in \mathbb{R}$ defined as

$$\nu_3^{cl}(x_3) \equiv \tau_\psi^{cl}(x_3) := -k_\psi \sin(2\psi) - k_{\omega_\psi}\omega_\psi, \tag{33}$$

which induces the closed loop vector field $\tilde{\mathbb{X}}_3 \ni x_3 \mapsto X_3^{cl}(x_3) := X_3(x_3, \tau_\psi^{cl}(x_3))$; and where we emphasize that $\tau_\psi^{cl}(0_2) = 0$ and that $\lim_{\psi\to\pm\pi/2} \tau_\psi^{cl}((\psi, \cdot)) = \mp\infty$ (we also note that the control law is continuous and periodic in $(\mathbb{R}\backslash\sim) \times \mathbb{R} \simeq \left(-\frac{\pi}{2}, \frac{\pi}{2}\right] \times \mathbb{R}$). It follows that for the (Lyapunov) function $\tilde{\mathbb{X}}_3 \ni x_3 \mapsto V_3(x_3) \geq 0$ defined as $V_3(x_3) := k_\psi(1 - \cos(2\psi)) + \omega_\psi^2$ it holds that $\tilde{\mathbb{X}}_3 \ni x_3 \mapsto W_3(x_3) := DV_3(x_3)X_3^{cl}(x_3)$ yields $W_3(x_3) = -2k_{\omega_\psi}\omega_\psi^2 \leq 0$. It follows from V_3 and W_3 that a solution $t \mapsto x_3(t)$ of $\dot{x}_3(t) = X_3^{cl}(x_3(t))$ converges to either the equivalence class $[0] = \{k\pi : k \text{ integer}\}$ (stable) or to the equivalence class $\left[\frac{\pi}{2}\right] = \{k\frac{\pi}{2} : k \text{ integer}\}$ (unstable). We emphasize that, with the choice of ψ (in (19)) that we made, the yaw control does not see a difference between the vehicles: i.e., if, for example, when seen from a top view, vehicle 1 points North w.r.t. vehicle 2, then that corresponds to the same yaw as if vehicle 2 points North w.r.t. vehicle 1. As such, the yaw control here performed is that of the *plane* containing the vertical direction, and the two vehicles when projected onto an horizontal plane (note that, indeed, the yaw of a *plane* does not see a difference in half rotations, justifying the introduced equivalence relation).

D. Complete control law

We are now in position of providing (8), and thus (9). Consider then the control laws (28), (31) and (33), and the corresponding sets (27), (30) and (32). The set $\tilde{\mathbb{X}} := \tilde{\mathbb{X}}_1 \times \tilde{\mathbb{X}}_2 \times \tilde{\mathbb{X}}_3$ provides then the domain of the control law ν^{cl} in (8), and we note that $\{z \in \mathbb{Z} : g(z) \in \tilde{\mathbb{X}}\} \subset \tilde{\mathbb{Z}}$. The control law u^{cl} in (9) can then be implemented yielding the closed loop vector field (10). Finally, we note that an inverse of g (in (25a)) exists when restricted to $\tilde{\mathbb{X}}$, i.e., there exists a g^{-1} such that $g^{-1}(g(z)) = z$ for all $z \in \{z \in \mathbb{Z} : g(z) \in \tilde{\mathbb{X}}\} \subset \tilde{\mathbb{Z}}$.

Theorem 2: Consider the system with vector field (6), and the control law (9), which yields the closed loop vector field (10). It follows that for any initial condition $z(0) \in \{z \in \mathbb{Z} : g(z) \in \tilde{\mathbb{X}}\} \subset \tilde{\mathbb{Z}}$, a solution of $t \mapsto z(t)$ of $\dot{z}(t) = Z^{cl}(t, z(t))$ is such that $z(t) \in \tilde{\mathbb{Z}}$ for all $t \geq 0$, $\lim_{t\to\infty}(p(t) - p^\star(t)) = 0_3$, $\lim_{t\to\infty} \theta(z_k(t)) = \theta^\star$ and $\lim_{t\to\infty} \psi(z_k(t)) = 0$ (with the functions θ and ψ in (18) and (19)).

Proof: Given the solution $t \mapsto z(t)$, one may compute $t \mapsto x(t) := (x_1(t), x_2(t), x_3(t)) := g(z(t))$ via the mapping g in (25a). Since $z(0) \in \left\{z \in \mathbb{Z} : g(z) \in \tilde{\mathbb{X}}\right\} \subset \tilde{\mathbb{Z}}$, it follows that $x(0) := g(z(0)) \in \tilde{\mathbb{X}} := \tilde{\mathbb{X}}_1 \times \tilde{\mathbb{X}}_2 \times \tilde{\mathbb{X}}_3$. As shown in Sections V-A–V-C, the control laws guarantee that $t \mapsto x(t)$ does not get arbitrarily close to the boundaries of $\tilde{\mathbb{X}}$, and thus, $t \mapsto z(t) = g^{-1}(x(t))$ does also not get arbitrarily close to the boundaries of $\tilde{\mathbb{Z}}$. This guarantees then that the control law (9) is always well defined. Moreover, it was also concluded in the same sections, that $\lim_{t\to\infty} p(t) - p^\star(t) = 0_3$ ($x_1 = (p, v, n, \omega)$), that $\lim_{t\to\infty} \theta(t) = \theta^\star$ ($x_2 = (\theta, \omega)$) and that $\lim_{t\to\infty} \psi(t) \in [0]$ or $\left[\frac{\pi}{2}\right]$ ($x_3 = (\psi, \omega)$; equivalence class $\left[\frac{\pi}{2}\right]$ is unstable), justifying the theorem's conclusions. ∎

In [22], one finds an extended model, where the quadrotrors are not assumed fully actuated, and control laws for the quadrotors' throttles are provided which preserve the cascaded structure of the vector field X_1 in (26a) (which is omitted here due to space constraints).

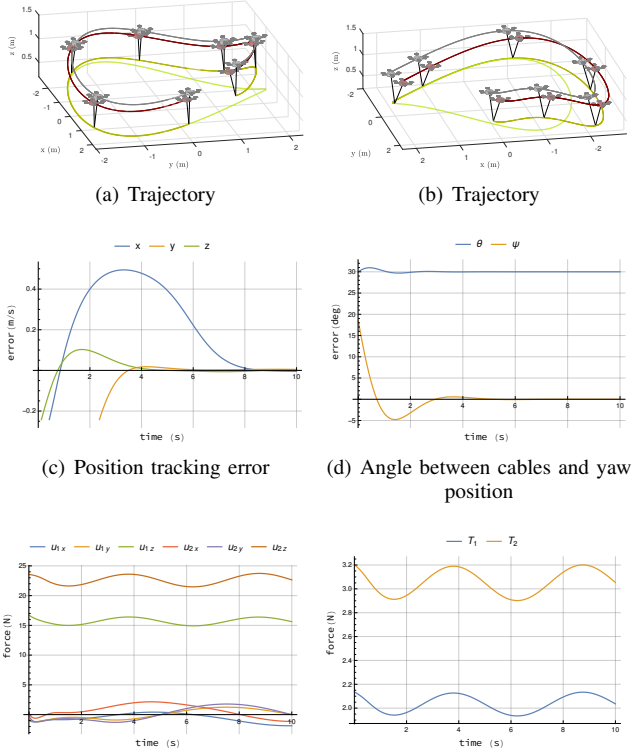

(a) Trajectory (b) Trajectory

(c) Position tracking error (d) Angle between cables and yaw position

(e) Input as computed from (23) (f) Tensions in cables

Fig. 3. Trajectory for vector field (6).

VI. Simulations

Consider the system quadrotors-load with parameters $m = 0.5\text{kg}$, $m_1 = 1.4\text{kg}$, $m_2 = 2.0\text{kg}$, $l_1 = 0.5\text{m}$, $l_2 = 0.7\text{m}$, $w_1 = 0.4$ and $w_2 = 0.6$. The desired position trajectory is $\mathbb{R}_{\geq 0} \ni t \mapsto p^\star(t) := (2\cos(\pi/5t), 2\sin(\pi/5t), 0.5 + 0.3\sin(\pi/2.5t)) \in \mathbb{R}^3$ m, and the desired angle between the cables is $\theta^\star = 30°$. The controllers and their gains are found in [22] (the control law (31) is that from [23]). For these choices, we provide a simulation in Fig. 3, as a solution $t \mapsto z(t) \in \bar{\mathbb{Z}}$ of (6) composed with the proposed control law (23) and with $\bar{z}(0) = (0_3, p_1, p_2, 0_9) \in \bar{\mathbb{Z}}$, with $p_1 \approx (0.05, 0.07, 0.49) \in \mathbb{R}^3$ and $p_2 \approx (-0.07, -0.10, 0.69) \in \mathbb{R}^3$. In Figs. 3(a)–3(b), one can visualize the quadrotors-load trajectory, and a visual inspection indicates the desired position is tracked. In Figs. 3(c), the position errors are shown, and one verifies that indeed the error position ($t \mapsto p(t) - p^\star(t)$) is steered to zero. In Figs. 3(d), the angle between the cables and the yaw position are shown, and one verifies that $t \mapsto \theta(z_k(t))$ converges to the desired angle $\theta^\star = 30°$, while $t \mapsto \psi(z_k(t))$ converges to 0. In Fig 3(e), the input computed from (23) is shown, and, finally, in Fig. 3(f) one can visualize the tensions in the cables $t \mapsto T_i(z(t), u_1^{cl}(t, z(t)), u_2^{cl}(t, z(t)))$; one verifies that those tensions are always positive, which means the cables are always taut. Recall from Remark 1 that, for a stationary desired trajectory, $T_1/T_2 = w_1/w_2 = 2/3$, and it can be seen in Fig. 3(f) that that is met approximately for non-stationary trajectories. Deriving precise conditions on the initial state that guarantee that the tensions remain positive has been left for future research. Also, simulations with non-fully actuated quadrotors are found in [22].

References

[1] AEROWORKS aim. Retrieved from http://www.aeroworks2020.eu/. September, 2016.

[2] F. Kendoul. Survey of advances in guidance, navigation, and control of unmanned rotorcraft systems. *Journal of Field Robotics*, 29(2):315–378, 2012.

[3] N. Michael, J. Fink, and V. Kumar. Cooperative manipulation and transportation with aerial robots. *Autonomous Robots*, 30(1):73–86, 2011.

[4] M. Orsag, C. M. Korpela, S. Bogdan, and P. Y. Oh. Hybrid adaptive control for aerial manipulation. *Journal of Intelligent & Robotic Systems*, 73(1):693–707, 2013.

[5] J.L.J. Scholten, M. Fumagalli, S. Stramigioli, and R. Carloni. Interaction control of an UAV endowed with a manipulator. In *IEEE International Conference on Robotics and Automation (ICRA)*, pages 4910–4915, May 2013.

[6] H. Lee, H. Kim, and H.J. Kim. Path planning and control of multiple aerial manipulators for a cooperative transportation. In *IEEE/RSJ International Conference on Intelligent Robots and Systems (IROS)*, pages 2386–2391, Sept 2015.

[7] G. Wu and K. Sreenath. Geometric control of multiple quadrotors transporting a rigid-body load. In *53rd IEEE Conference on Decision and Control*, pages 6141–6148, Dec 2014.

[8] T. Lee. Geometric control of multiple quadrotor UAVs transporting a cable-suspended rigid body. In *Conference on Decision and Control*, pages 6155–6160. IEEE, 2014.

[9] P. O. Pereira, R. Zanella, and D. V. Dimarogonas. Decoupled design of controllers for aerial manipulation with quadrotors. In *2016 IEEE/RSJ International Conference on Intelligent Robots and Systems (IROS)*, pages 4849–4855, Oct 2016.

[10] M. E. Guerrero, D. A. Mercado, R. Lozano, and C. D. Garcia. Passivity based control for a quadrotor UAV transporting a cable-suspended payload with minimum swing. In *2015 54th IEEE Conference on Decision and Control (CDC)*, pages 6718–6723, Dec 2015.

[11] M. Bisgaard, J. D. Bendtsen, and A. L. Cour-Harbo. Modeling of generic slung load system. *Journal of guidance, control, and dynamics*, 32(2):573–585, 2009.

[12] M. Bernard and K. Kondak. Generic slung load transportation system using small size helicopters. In *International Conference on Robotics and Automation*, pages 3258–3264. IEEE, 2009.

[13] M. Bisgaard, A. Cour-Harbo, E. N. Johnson, and J. D. Bendtsen. Vision aided state estimator for helicopter slung load system. *17th IFAC Symposiumon Automatic Control in Aerospace*, 2007.

[14] I. Palunko, P. Cruz, and R. Fierro. Agile load transportation. *IEEE Robotics Automation Magazine*, 19(3):69–79, 9 2012.

[15] K. Sreenath, N. Michael, and V. Kumar. Trajectory generation and control of a quadrotor with a cable-suspended load - A differentially-flat hybrid system. In *International Conference on Robotics and Automation*, pages 4888–4895. IEEE, 2013.

[16] É. Servais, H. Mounier, and B. d'Andréa Novel. Trajectory tracking of trirotor UAV with pendulum load. In *20th International Conference on Methods and Models in Automation and Robotics (MMAR)*, pages 517–522, Aug 2015.

[17] T. Lee, K. Sreenath, and V. Kumar. Geometric control of cooperating multiple quadrotor UAVs with a suspended payload. In *Conference on Decision and Control*, pages 5510–5515. IEEE, 2013.

[18] P. Pereira, M. Herzog, and D. V. Dimarogonas. Slung load transportation with single aerial vehicle and disturbance removal. In *Mediterranean Conference on Control and Automation*, pages 671–676, 2016.

[19] M. Bisgaard, A. Cour-Harbo, and J. D. Bendtsen. Adaptive control system for autonomous helicopter slung load operations. *Control Engineering Practice*, 18(7):800 – 811, 2010. Special Issue on Aerial Robotics.

[20] S. Dai, T. Lee, and D. S. Bernstein. Adaptive control of a quadrotor UAV transporting a cable-suspended load with unknown mass. In *Conference on Decision and Control*, pages 6149–6154. IEEE, 2014.

[21] M. Hua, T. Hamel, P. Morin, and C. Samson. Introduction to feedback control of underactuated VTOL vehicles: A review of basic control design ideas and principles. *Control Systems*, 33(1):61–75, 2013.

[22] P. O. Pereira and D. V. Dimarogonas. Mathematica files used in obtaining the manuscript's results. In *https://github.com/KTH-SML/control-framework-for-slung-load-transportation-with-two-aerial-vehicles.git*.

[23] P. O. Pereira and D. V. Dimarogonas. Lyapunov-based generic controller design for thrust-propelled underactuated systems. In *European Control Conference*, pages 594–599, 2016.